KSME

Springer

Journal of Mechanical Science and Technology 34 (9) 2020

Original Article
DOI 10.1007/s12206-020-0818-8

Keywords:
· Centrifugal pump
· Clearance flow
· Frequency spectra
· Numerical calculation
· Pressure fluctuation

Correspondence to:
Xiaoping Chen
chenxp@zstu.edu.cn

Citation:
Zheng, L., Chen, X., Zhang, W., Zhu, Z., Qu, J., Wang, M., Ma, X., Cheng, X. (2020). Investigation on characteristics of pressure fluctuation in a centrifugal pump with clearance flow. Journal of Mechanical Science and Technology 34 (9) (2020) 3657~3666.
http://doi.org/10.1007/s12206-020-0818-8

Received February 26th, 2020
Revised May 3rd, 2020
Accepted June 24th, 2020

† Recommended by Editor Yang Na



# Investigation on characteristics of pressure fluctuation in a centrifugal pump with clearance flow

**Lulu Zheng[1], Xiaoping Chen[2], Wei Zhang[2], Zuchao Zhu[2], Jinglei Qu[1], Mengmeng Wang[1], Xiaojie Ma[1] and Xueli Cheng[1]**

[1]Faculty of Mechanical Engineering, Henan Institute of Technology, Xinxiang, Henan 453003, China, [2]National-Provincial Joint Engineering Laboratory for Fluid Transmission System Technology, Zhejiang Sci-Tech University, Hangzhou, Zhejiang 310018, China

**Abstract** Clearance flow has great impact on pressure fluctuation of centrifugal pumps. Numerical calculations are performed to study the pressure fluctuation characteristics of centrifugal pump with wear ring clearance, especially in the regions of interaction between main flow and clearance flow (IMC) and clearance. The accuracy of numerical calculations is illustrated by comparing the experiments of performance and pressure fluctuation. Results show that, in clearance region the pressure fluctuation is still governed by blade passing frequency ($f_{BPF}$). Its amplitude of dominate frequency of pressure fluctuation becomes larger as the probe approaches the impeller exit. In IMC region, the pressure fluctuation at impeller outlet is dominated by $f_{BPF}$. However, the dominate frequency at the entrance of impeller is less than $f_{BPF}$. In addition, as the flow rate increased, the amplitude of dominate frequency of pressure fluctuation increases at impeller entrance, whereas an inverse trend is observed at wear ring clearance region.

## 1. Introduction

Strong pressure fluctuation has important influence on the stability and safety of centrifugal pump operation, which is widely used as key equipment in aerospace, hydraulic engineering, petrochemical and coal chemical industries [1-7]. Unsteady pressure fluctuation, which is closely associated with the main flow and clearance flow, directly affects the pump comprehensive performance.

A large number of research work has been done on pressure fluctuation of the centrifugal pumps, which is mainly focusing on the main flow [8-22]. Spence and Amaral-Teixeira [8] analyzed the pressure geometric parameters on the pressure fluctuation of a pump, by extracting the date from 15 monitoring points. Intense pressure fluctuation between impeller and volute may be troublesome during the operation of the pump. Thus, it is significantly to reduce the strong pressure fluctuation in order to ensure the stability and safety of centrifugal pump operation. Zhang et al. [14] compared the pressure fluctuation characteristics in slope volute pump and conventional spiral volute pump, respectively. The results demonstrate that the pressure fluctuation intensity is reduced in the pump with slope volute. Gao et al. [16] studied the influence of blade trailing edge shape on the pressure fluctuation characteristics of a centrifugal pump. The results show that proper blade profile can effectively reduce the amplitude of dominate frequency of pressure fluctuation.

It is worth noting that none of the above studies considered clearance flow, and its effect on characteristics of pressure fluctuations is usually ignored in numerical calculations. Clearance flow, which exists in the actual operation of the centrifugal pump, causes flow loss, destroys the orderly flow at impeller inlet, and thus affects the distribution of unsteady pressure fluctuation. Therefore, it is necessary to study the pressure fluctuation characteristics in the pump including clearance flow [23-33]. Cao et al. [25] analyzed the relationship between clearance and pump

efficiency. Research shows that the effect of clearance flow on pump efficiency cannot be neglected. Feng et al. [28] studied the pressure fluctuation distribution in the axial flow pump including the clearance flow and found that the clearance flow causes an increase in the pulsation intensity of the impeller. Zhang et al. [29] analyzed the effect of different tip clearance on the pressure fluctuation within a pump. In recent years, Liu et al. [31] studied the effects of different clearance sizes on unsteady flow in the centrifugal pump and obtained detailed flow characteristics in the centrifugal pump. Cao et al. [32] studied the distribution characteristics of pressure pulsation in a centrifugal pump including the clearance flow. The results show that the clearance flow has a great influence on the main flow in the pump, and its influence should be considered.

A large number of research work has been done on characteristics of pressure fluctuation in the centrifugal pumps without considering clearance flow, and the research areas are concentrated on the impeller outlet, volute wall surface, etc. However, the research on performance and pressure fluctuation of centrifugal pump by clearance flow is relatively few, when considering the clearance flow. The studies on the clearance flow within centrifugal pump is insufficient and it is not clear how it affects the pressure pulsation in the clearance area of the pump. Furthermore, clearance flow causes the interaction between the main flow and clearance flow (IMC) at impeller inlet and outlet. The pressure fluctuation characteristics within IMC region is seldom analyzed and thus its pressure fluctuation characteristics must be examined in detail. Therefore, it is meaningful to study how the clearance flow affects the pressure fluctuation within centrifugal pump.

The main work of current research is to study the effect of clearance flow on pressure fluctuation within centrifugal pump at different discharge. The structure of this paper is as follows. Sec. 2 shows the numerical considerations. The results and discussions are discussed in Sec. 3. Sec. 4 presents the conclusions of this paper at last.

## 2. Numerical considerations

### 2.1 Geometric model

The centrifugal pump analyzed in this paper is a single stage single-entry centrifugal pump. The geometric structure of the centrifugal pump is shown in Fig. 1, including impeller, front pump chamber, back pump chamber and volute. In addition, the position of the wear ring clearance is also marked in detail in Fig. 1. The flow and the head under design flow rate are $Q_d$ = 45 $m^3/h$ and $H_d$ = 30.9 m, respectively. Table 1 shows the main values and parameters of the pump.

### 2.2 Numerical methods and wear ring mesh validation

Governing equations involved in all numerical calculations are unsteady three-dimensional incompressible RANS equations. The commercial CFD code ANSYS-Fluent was used to solve the governing equations. The steady calculation of the full flow field in centrifugal is performed at initial. The unsteady numerical calculation of centrifugal pump is based on the result of the steady calculation. The time step of the unsteady calculation is $\Delta t = 5.575\times10^{-5}$ s, which corresponds to the time that the impeller rotates by one degree. More details about computational grids, turbulence model, boundary conditions and time step size verification can be taken from our previous work [30].

The mesh has an important influence on the accuracy of the numerical calculations. Therefore, the structure mesh is applied in this calculation. The quality of the wear ring mesh has a great impact on the local internal flow field of the centrifugal pump. Thus, four sets of the mesh tests are conducted for the wear ring clearance region. Fig. 2 shows the turbulent kinetic energy distribution on the center line of wear ring clearance with different mesh nodes at design flow rate. The results show that the turbulent kinetic energy distribution with 3 nodes is obviously different from the other three groups in the magnitude and distribution tendency. It is indicated that when the number of mesh nodes increases to 21, the calculation results tend to be consistent. Fig. 3 shows the distribution of wear ring flow rate versus the mesh nodes at design flow rate, and presents the structured mesh of the wear ring. Results show that the wear ring flow rate is different under four mesh nodes, and the variation of flow rate with the mesh nodes is relatively small. At 21 mesh nodes, the relative variation of the flow rate is

Table 1. Geometric parameters and values.

| Parameters | Unit | Symbol | Value |
|---|---|---|---|
| Head | m | $H_d$ | 30.9 |
| Flow rate | $m^3/h$ | $Q_d$ | 45 |
| Rotation speed | r/min | $n_d$ | 2900 |
| Efficiency | % | $\eta$ | 64.5 |
| Specific speed | - | $n_s$ | 90 |
| Number of blades | - | $Z$ | 6 |
| Diameter of impeller inlet | mm | $D_1$ | 86 |
| Diameter of impeller outlet | mm | $D_2$ | 161 |
| Wear ring clearance length | mm | $l$ | 13 |
| Wear ring clearance | mm | $b$ | 0.35 |

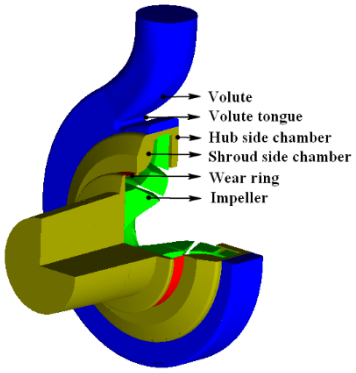


Fig. 1. Geometry diagram of centrifugal pump.

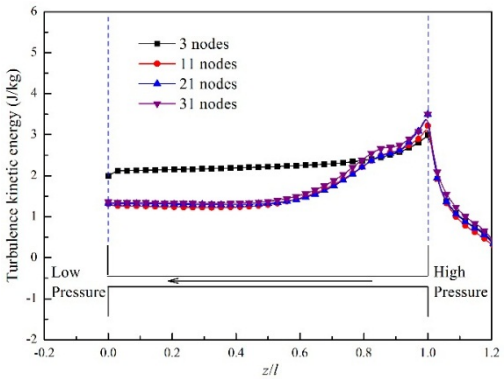


Fig. 2. Turbulent kinetic energy distribution on the center line of wear ring.

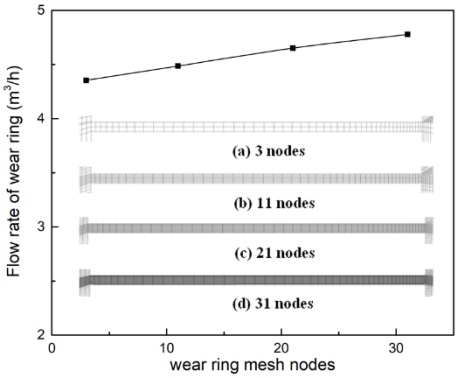


Fig. 3. Wear ring flow rate versus the mesh nodes.

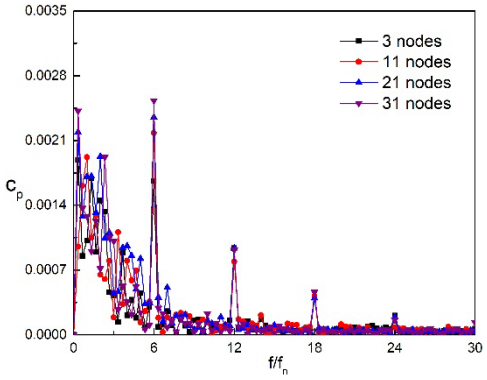


Fig. 4. Pressure fluctuation spectra of wear ring versus the mesh nodes at design flow rate.

within 3 % and reaches the minimum variation value.

Fig. 4 shows the pressure fluctuation of wear ring versus the mesh nodes at design flow rate. Results show that at different mesh nodes the blade passing frequency $f_{BPF}$ and its harmonic frequency are captured in the frequency domain distribution. The overall distribution trend of pressure spectrum is similar at different mesh nodes, but the amplitude is different to some extent. At 21 mesh nodes, the relative variation of the amplitude of $f_{BPF}$ is relatively small. Thus, considering the calculation time and calculation accuracy, the mesh case with 21 wear ring mesh nodes is applied in the final calculation. The total mesh

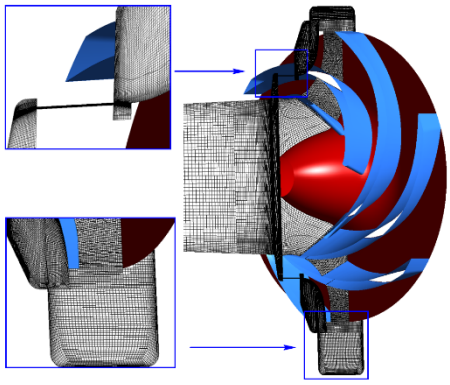

Fig. 5. Mesh view of centrifugal pump.

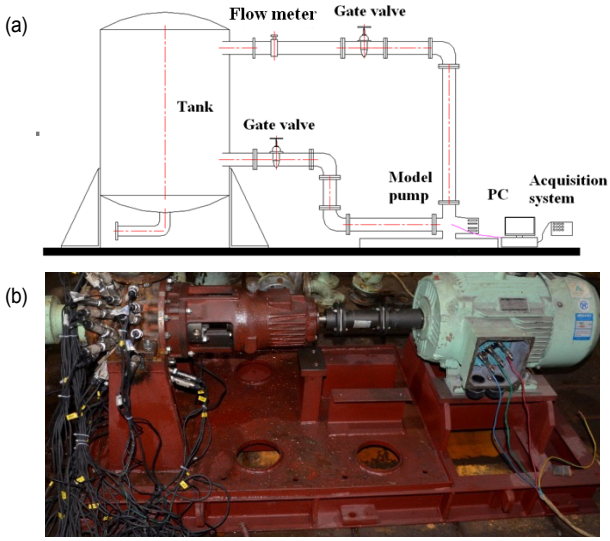


Fig. 6. Experiment rig: (a) schematic diagram; (b) pump.

numbers are 6.98 million, in which the mesh number of impeller, volute, pump chamber, inlet pipe and outlet pipe are 1413918, 1327226, 3819421, 216732 and 204533, respectively. Fig. 5 shows the detail mesh of the pump.

## 2.3 Calculation accuracy validation

The experiments are conducted in Zhejiang Sci-Tech University at National-Provincial Joint Engineering Laboratory for Fluid Transmission System Technology [30]. Fig. 6 shows the experiment rig of the centrifugal pump including tank, sensors, centrifugal pump and data collection and handling system. The rotational speed was measured by using a photoelectric tachometer. The sensor ranges were -0.1 to 0.1 MPa and 0 to 1.0 MPa. More details about the experiment system can be taken from our previous work [30].

Fig. 7(a) shows comparison between the unsteady numerical results of centrifugal pump and the experimental results. At design flow rate, the head relative tolerance and the efficiency relative tolerance is 2.86 % and 2.59 %. The maximum deviation between the head curve and the efficiency curve of calcu-

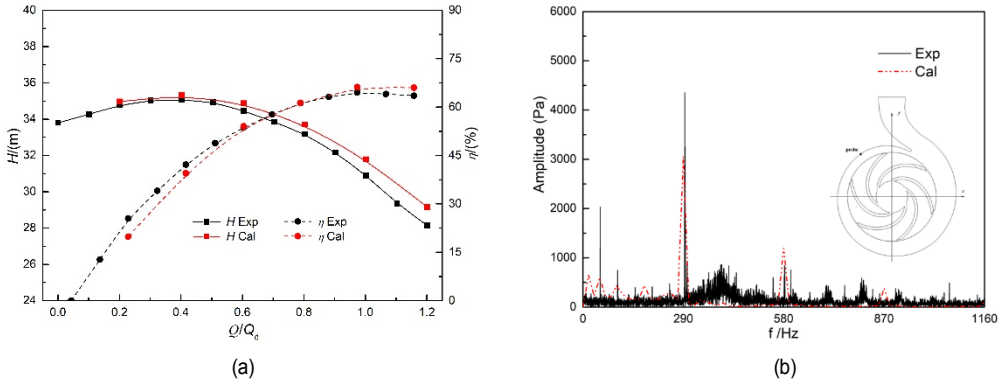


Fig. 7. (a) Performance curves; (b) frequency spectra of centrifugal pump.

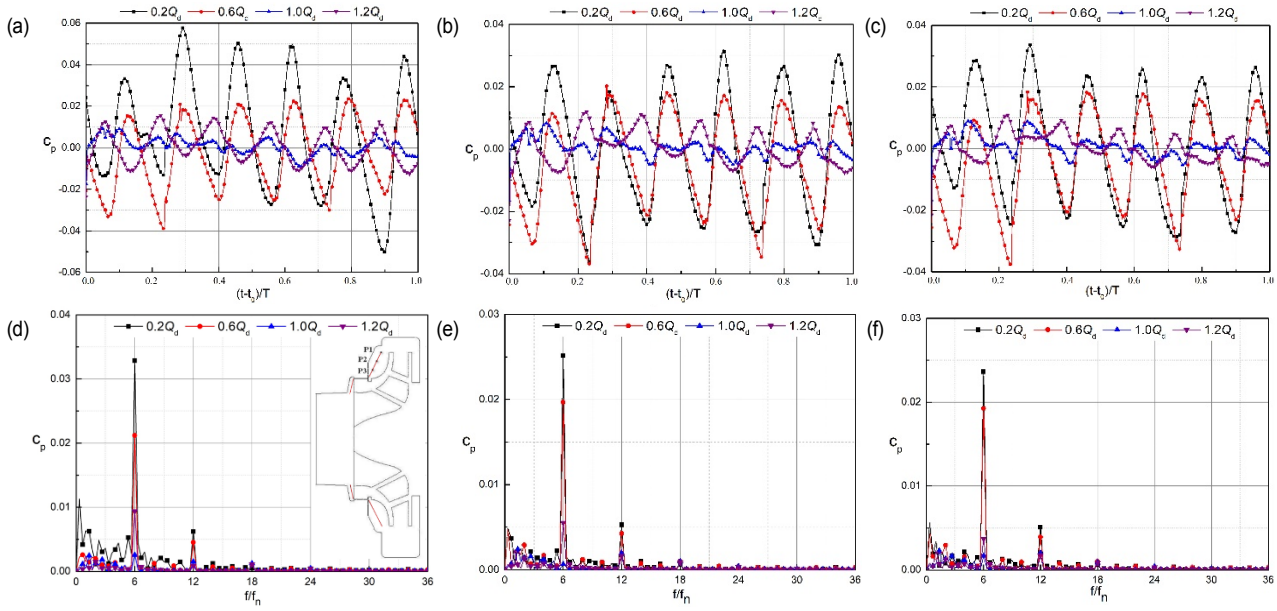


Fig. 8. Pressure fluctuation at (a) P1; (b) P2; (c) P3, frequency spectra at (d) P1; (e) P2; (f) P3.

lation results and experiment results are within 4 % under different working conditions. In the experiment of pressure fluctuation, limited to the influence of factors such as pump geometry, sensor size, layout scheme, etc., the measuring point near tongue, which is shown in Fig. 7(b), is extracted and analyzed. Fig. 7(b) presents the frequency spectra at selected probe under design flow rate. Results show that the calculation results are consistent with the experiment results in the distribution trend, with small differences in amplitude. In total, the difference between numerical calculation results and experiment results is very small, which indicates the accuracy of the calculation results.

## 3. Results and discussions

### 3.1 Characteristics of pressure fluctuation within clearance region

#### 3.1.1 Pressure fluctuation in front cavity

The pressure fluctuation coefficient is defined as

$$c_p = \frac{p - \overline{p}}{0.5\rho u^2} \tag{1}$$

where $p$ stands for static pressure, $\overline{p}$ stands for time average static pressures of the probes, and $u$ stands for impeller circumferential velocity. Pressure fluctuation and frequency spectra is presented in Fig. 8, and the probes are marked in Fig. 8(d). It is noticed that the pressure distribution of probes presents a periodic distribution. At $0.2Q_d$ and $0.6Q_d$, the pressure fluctuation signal at the probe has six peaks and valleys, respectively. At $1.0Q_d$ and $1.2Q_d$, the pressure fluctuation periodic regulation at each probe is weakened to some extent. For any probe, the pressure fluctuation amplitude is the largest at small working condition. As the flow rate increases, the amplitude of pressure fluctuation decreases gradually. At design condition, the pressure fluctuation is minimal. At $1.2Q_d$ flow rate, the amplitude of pressure fluctuation at the probe increased slightly, but it was still much lower than the pulsation intensity

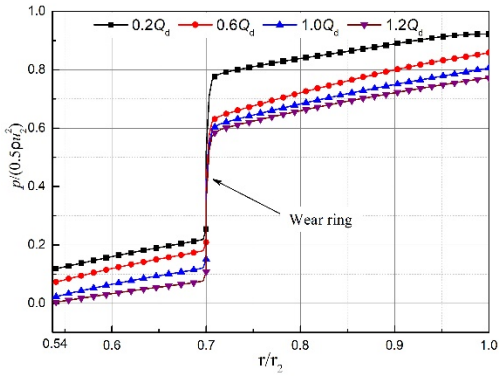


Fig. 9. Distribution of pressure in radial direction of front cavity.

under low flow rate. Figs. 8(d)-(f) show the pressure frequency domain diagram. At low flow rate, broadband signals appear in low frequency band, which may be caused by unsteady flow such as vortex in the cavity. At different flow rates, the dominate frequency at any probe is blade passing frequency ($f_{BPF}$) and its multiplier, and the spectrum signal decays rapidly. It indicates that the pressure fluctuation of the front cavity is dominated by rotor-stator interaction. By comparing the amplitude of dominate frequency of pressure fluctuation at each probe, it is found that the maximum amplitude of dominate frequency of pressure fluctuation decreases as the flow rate increases, and reaches the minimum value under design flow rate. At large working condition, the amplitude which is corresponding to the dominate frequency of pressure fluctuation increases. At low flow rate, the amplitude of dominate frequency of pressure fluctuation at probe P1 is largest. It indicates that in this area the intensity of pressure fluctuation is relatively high, which is greatly affected by the volute tongue.

In conclusion, in the front cavity the pressure fluctuations at probes have similar distribution pattern, and the pressure fluctuation is still dominated by rotor-stator interaction. Besides, it is found that the pressure fluctuation becomes more intense at front cavity entrance. The amplitude of dominate frequency of pressure fluctuation decreases as the flow rate increased to design flow rate, and then increases with the flow rate.

Fig. 9 shows the distribution of average pressure in the radial direction of front cavity monitoring line. The abscissa represents the dimensionless radial radius, 0.54 indicating the outlet of the front cavity, 0.7 corresponding to the wear ring, and 1.0 corresponding to the inlet of the front cavity. It is found that, pressure distribution in the front cavity is similar under different flow rates. The largest average pressure is obtained at the front cavity entrance. The average pressure decreases continuously as the radius decreases. At wear ring, its geometry obstructs the clearance flow, resulting in a rapid decrease in pressure. As the radius decreases further, the pressure decreases continuously and reaches a minimum value near the front cavity outlet. The largest pressure inside the pump cavity is obtained at $0.2Q_d$ flow rate, but the pressure value decreased as the flow rate increases.

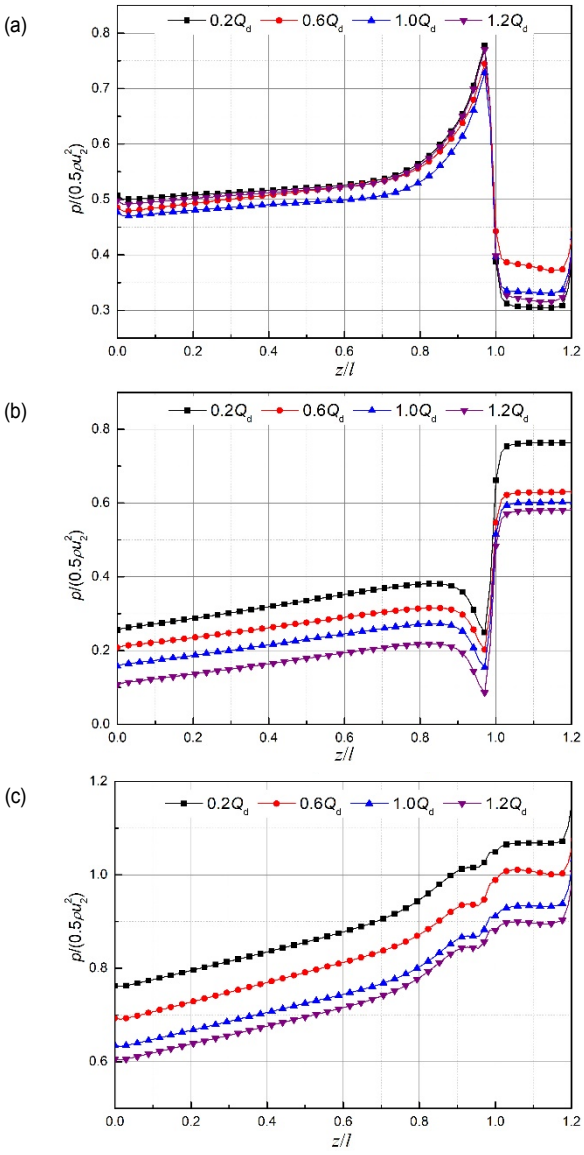


Fig. 10. Distribution of pressure on the center line of the wear ring: (a) dynamic; (b) static; (c) total pressures.

### 3.1.2 Pressure fluctuation in wear ring

Fig. 10 presents the pressure distribution of the center line in the wear ring, and the data is the average value of four lines uniformly distributed in the circumferential direction of the wear ring at a certain moment. The abscissa indicates the dimensionless wear ring position, 0 indicates the wear ring exit, 1 indicates the wear ring inlet, and 1.2 indicates the impeller front cover. The layout of the wear ring structure is denoted in Fig. 11(b).

It is found that the flow parameters in wear ring have the similar distribution at different working conditions. In Figs. 10(a) and (b), the dynamic and static pressure are almost unchanged from 1.2 to 1.0 region. At 1.0 position, both dynamic pressure and static pressure suddenly changed. The difference was that the fluid dynamic pressure increased rapidly to the

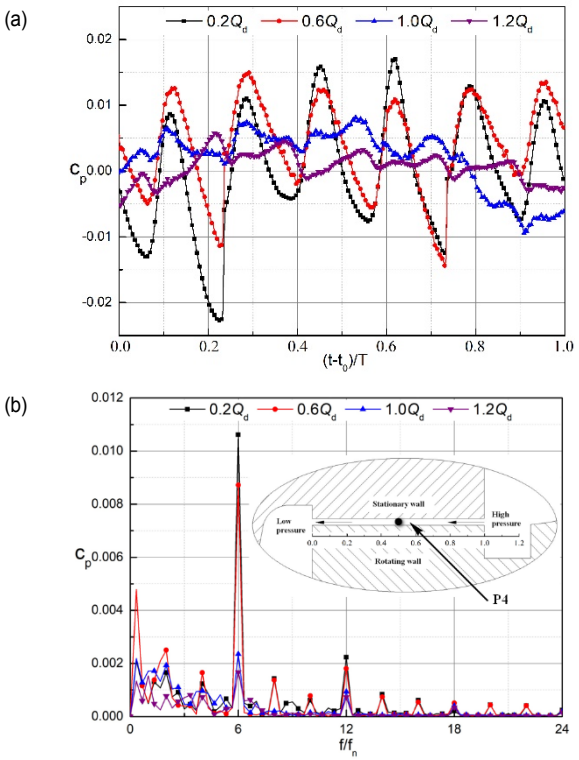


Fig. 11. (a) Pressure fluctuation; (b) pressure frequency spectra at selected monitor point.

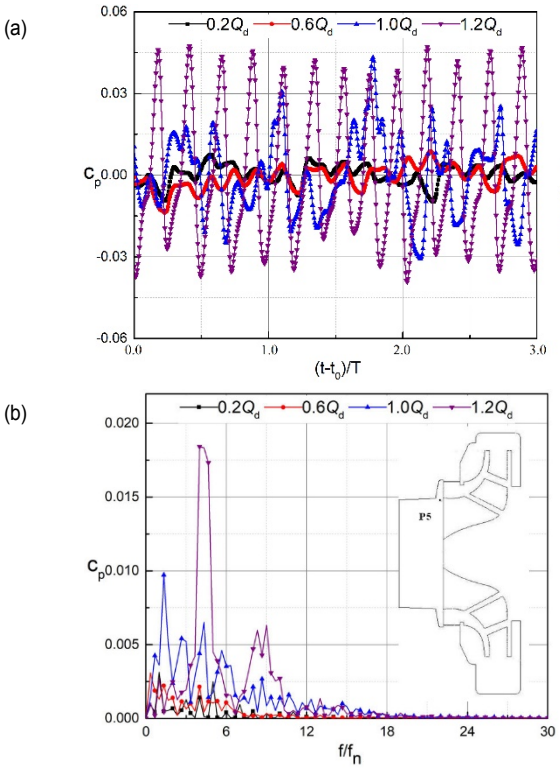


Fig. 12. Distributions of (a) pressure fluctuation; (b) pressure frequency spectra at impeller inlet.

maximum value, while the static pressure decreased sharply to the minimum value. In the region from 1.0 to 0.8, the dynamic pressure decreased slightly, but is still higher than the dynamic pressure before wear ring entrance; the static pressure increased, but is still lower than the static pressure before the wear ring entrance. From 0.8 to 0, the dynamic pressure has only a slight decrease, but the static pressure decreases greatly along the flow direction in wear ring clearance. The total pressure distribution is presented in Fig. 10(c). From, 1.2 to 0, the total fluid pressure shows a decreasing trend. It suggests the continuously decrease of the total fluid energy. At different working conditions, the total pressure distribution remains unchanged. The total pressure is the largest at $0.2Q_d$, and as the flow rate increases it decreases instead.

At the wear ring entrance, the sudden decrease of the geometry causes a rapid increase in the fluid velocity. This leads to a sudden increase in dynamic pressure and a rapid decrease in static pressure. The dynamic and static pressure remain the original distribution under different working conditions. In contract, the change on static pressure is significantly higher than that of dynamic pressure. On the whole, the total pressure decreases gradually along the flow direction in the wear ring clearance. This phenomenon consistent good with the theoretical and simulation findings with analytical model of Bruurs et al. [34, 35].

Fig. 11 shows pressure fluctuation and frequency spectra at selected probe of wear ring under various flow rate. The pressure distribution shows evident periodicity at $0.2Q_d$ and $0.6Q_d$. The pressure fluctuation periodicity and intensity decrease in turn as the flow rate increases. The $f_{BPF}$ is found in distribution of frequency spectra. Besides, other frequency signals including axial frequency, are also found. The signal at low frequency is more complicated. The sudden change in flow parameters of wear ring clearance and the interaction between the dynamic side and static side of the wear ring lead to more complicated pressure fluctuation in the wear ring. The largest amplitude of dominate frequency of pressure fluctuation is achieved at $0.2Q_d$, which indicating the strongest intensity of the pressure fluctuation. As flow rate increases, the amplitude of dominate frequency of pressure fluctuation in the wear ring clearance decreases along with the flow rate and its minimum value is obtained at $1.2Q_d$.

In summary, the characteristics of pressure fluctuation in wear ring are largely affected by the rotor-stator interaction. Meanwhile, it is subject to a combination of high energy leakage flow of the wear ring, dynamic and static interference of the wear ring, and unsteady flow of the clearance flow. The dominate frequency of pressure fluctuation in wear ring clearance is $f_{BPF}$, and its amplitude decreases with the increase of the flow rate.

### 3.2 Characteristics of pressure fluctuation within IMC region

When the clearance flow exists, the high-pressure flow from

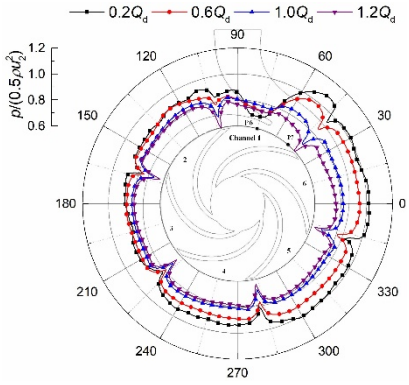


Fig. 13. Distribution of pressure on circumference at the outlet of impeller.

the impeller outlet will partly circulate from the cavity through the wear ring to impeller inlet and cause the flow loss. Clearance flow causes the interaction between main flow and clearance flow (IMC) at the impeller inlet and impeller outlet and its pressure fluctuation characteristics must be examined in detail.

### 3.2.1 Pressure fluctuation at impeller entrance

At the impeller inlet, the orderly flow is disrupted by the wear ring leakage flow. Pressure fluctuation and frequency spectra at impeller inlet is presented in Fig. 12. The pressure fluctuation is relatively small at $0.2Q_d$ and $0.6Q_d$, which is clearly shown in Fig. 12(a). As the flow increases continuously, pressure fluctuations increase obviously and presents periodicity to some extent, especially at $1.2Q_d$. However, there are 13 peaks and troughs appear in the three impeller rotation cycles. It is found in Fig. 12(b) that, the dominate frequency is small and much lower than $f_{BPF}$ at low working condition. The dominate frequency increases gradually with the increase of the flow rate, but it is still lower than $f_{BPF}$. At $1.2Q_d$, the dominate frequency is $0.67f_{BPF}$. It is found that the dominate frequency which corresponding to the pressure fluctuation at various flow rate is different, and its amplitude increases significantly as the flow rate increases.

### 3.2.2 Pressure fluctuation at impeller outlet

Fig. 13 presents the distribution of pressure on circumference at the outlet of impeller. In general, the pressure at the impeller outlet is the largest at small working condition. At the impeller outlet the pressure decreases gradually as the flow increases, and the pressure is the smallest at $1.2Q_d$. At $0.2Q_d$, pressure increases from channel 1 along the impeller rotating direction and the pressure fluctuation is the most significant among the various working condition. When flow rate grows bigger, pressure fluctuation at impeller outlet gradually weakens, especially at $1.0Q_d$ and $1.2Q_d$. There are six valleys at the circumferential of the impeller, which corresponding to blades trailing edge. It is concluded that pressure fluctuation is largest at the outlet of the channel 1, especially at $0.2Q_d$. The maximum pressure is obtained at the blade trailing edge, which is approaching to the tongue, and obtains minimum pressure

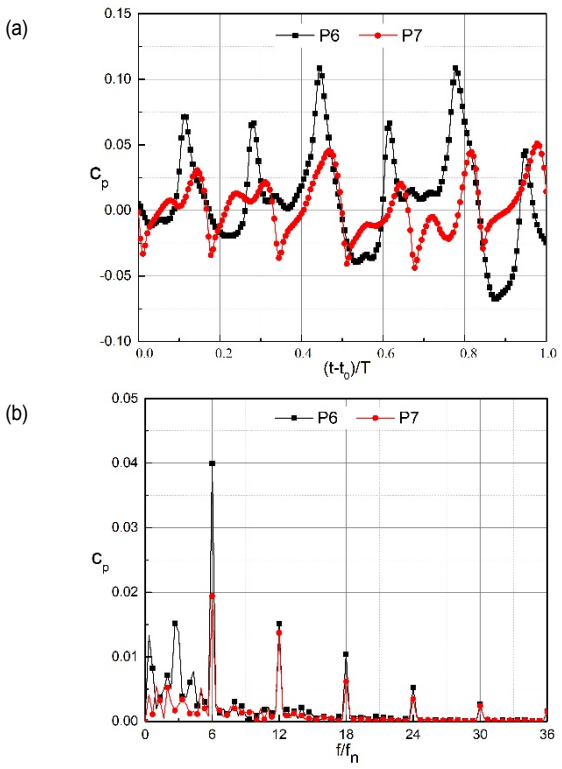


Fig. 14. Distributions of (a) pressure fluctuation; (b) pressure frequency spectra at selected probes at $0.2Q_d$.

near the tongue. The distribution of pressure is relatively smooth at other channels.

According to Fig. 13, the distribution of pressure fluctuation at points P4 and P5 at $0.2Q_d$ flow rate is obviously different, so the distribution of pressure fluctuation and frequency domain diagrams of points P4 and P5 at $0.2Q_d$ are presented in Fig. 14. The pressure fluctuation of the two points show obvious periodic fluctuation, as is shown in Fig. 14(a). However, there are difference in the amplitude of the peak and trough for P4 and P5, respectively. In contrast, the pressure fluctuation at point P4 is more irregular than that at P5. At the same time, the magnitude of peak and trough difference at point 4 is significantly higher than the result at point 5. The $f_{BPF}$ is still the dominant frequency of the pressure fluctuation in Fig. 14(b). Meanwhile, there are also $Mf_{BPF}$ frequencies appeared in the pressure spectra distribution for the two probes ($M$ stands for positive integer). In addition, it is also found that the amplitude of dominate frequency of pressure fluctuation at P4 in the frequency domain is higher than that of P5, which is definitely twice the amplitude of P5. This phenomenon has close connection with the relative position of probe to the volute tongue.

## 4. Conclusions

We perform numerical simulation and experiments of centrifugal pump with wear ring clearance at different discharge to study the characteristics of pressure fluctuation. The reliability

of numerical calculation including the pressure fluctuation are validated by the experimental data. The behavior of pressure fluctuation within the clearance area is studied. Besides, the characteristics of pressure fluctuation in IMC region, which is directly affect by the clearance flow, is also analyzed carefully. The major findings of this paper are concluded below.

Pressure fluctuation characteristics within clearance region: In the front cavity, rotor-stator interaction dominates the distribution of pressure fluctuations. The closer to the impeller outlet, the more intense the pressure fluctuation is, especially under low working condition. In wear ring, rotor-stator interaction still dominates the distribution of pressure fluctuations. At the wear ring entrance, the static and dynamic pressure is completely opposite, the static pressure decreased suddenly and the dynamic pressure increased sharply.

Pressure fluctuation characteristics within IMC region: at the entrance of impeller, the dominate frequency grows with the flow, but it is still less than $f_{BPF}$. Its pressure fluctuation is influenced not only by rotor-stator interaction, but also by the interaction between main flow and wear ring leakage. At the outlet of impeller, the pressure distribution along the circumference is most nonuniform at the channel corresponding to tongue. This phenomenon becomes more significant under small flow conditions. The comparison of pressure fluctuation suggests that the intensity of pressure near the tongue is greater.

The influence of flow rate on the characteristics of dominate frequency of pressure fluctuation is concentrated at its amplitude. The amplitude of dominate frequency decreases as the flow rate increased to design flow rate, then increases with flow rate in front cavity. However, the amplitude of dominant frequency at impeller entrance and wear ring clearance shows a monotonous change as the flow rate increased, the former increases and the latter decreases.

## Acknowledgments

This work is performed with the support and under the auspices of the National Natural Science Foundation of China (51536008 and 51976198), the Public Projects of Zhejiang Province (LGG19E060006), the Key Research and Promotion Special Funding Project of Henan Province (192102210222, 202102210286), and Research Foundation for Talented Scholars of Henan Institute of Technology (KQ1861).

## Nomenclature

$c_p$ : Pressure fluctuation coefficient (–)
$b$ : Wear ring clearance (mm)
$D$ : Impeller diameter (mm)
$IMC$ : Interaction between main flow and clearance flow
$l$ : Clearance length of wear ring (mm)
$H$ : Head (m)
$\eta$ : Pump efficiency (%)
$n$ : Rotation speed (r/min)
$n_s$ : Specific speed (-)
$p$ : Static pressure (Pa)
$Q$ : Flow rate ($m^3/h$)
$u$ : Impeller circumferential velocity (m/s)
$Z$ : Blade number (–)

### Subscripts

$1$ : Inlet of impeller
$2$ : Outlet of impeller
$d$ : Design flow rate

### Superscripts

$\bar{}$ : Time average

## References

[1] J. F. Gülich, *Centrifugal Pumps*, Berlin: Springer (2008).
[2] X. P. Chen, Z. C. Zhu, H.-S. Dou and L. Yi, Large eddy simulation of energy gradient field in a centrifugal pump impeller, *Proceedings of the Institution of Mechanical Engineers, Part C: Journal of Mechanical Engineering Science*, 233 (11) (2019) 4047-4057.
[3] W. X. Ye, R. F. Huang, Z. W. Jiang, X. J. Li, Z. C. Zhu and X. W. Luo, Instability analysis under part-load conditions in centrifugal pump, *Journal of Mechanical Science and Technology*, 33 (1) (2019) 269-278.
[4] X. J. Li, P. L. Gao, Z. C. Zhu and Y. Li, Effect of the blade loading distribution on hydrodynamic performance of a centrifugal pump with cylindrical blades, *Journal of Mechanical Science and Technology*, 32 (3) (2018) 1161-1170.
[5] H. Y. Cheng, X. R. Bai, X. P. Long, B. Ji, X. X. Peng and M. Farhat, Large eddy simulation of the tip-leakage cavitating flow with an insight on how cavitation influences vorticity and turbulence, *Applied Mathematical Modelling*, 77 (2020) 788-809.
[6] L. W. Tan, W. D. Shi, D. S. Zhang, C. Wang, L. Zhou and E, Mahmoud, Numerical and experimental investigations on the hydrodynamic radial force of single-channel pumps, *Journal of Mechanical Science & Technology*, 32 (10) (2018) 4571-4581.
[7] L. Zhou, W. H. Wang, J. W. Hang, W. D. Shi, H. Yan and Y. Zhu, Numerical investigation of a high-speed electrical submersible pump with different end clearances, *Water*, 12 (4) (2020) 1116.
[8] R. Spence and J. Amaral-Teixeira, A CFD parametric study of geometrical variations on the pressure pulsations and performance characteristics of a centrifugal pump, *Computers & Fluids*, 38 (6) (2009) 1243-1257.
[9] J. J. Feng, F.-K. Benra and H. J. Dohmen, Investigation of periodically unsteady flow in a radial pump by CFD simulations and LDV measurements, *Journal of Turbomachinery*, 133 (1) (2011) 011004.
[10] Z. F. Yao, F. J. Wang, L. X. Qu, R. F. Xiao, C. L. He and M. Wang, Experimental investigation of time-frequency characteristics of pressure fluctuations in a double-suction centrifugal pump, *ASME Journal of Fluids Engineering*, 133 (10) (2011)

101303.
[11] B. Gao, P. M. Guo, N. Zhang, Z. Li and M. G. Yang, Unsteady pressure pulsation measurements and analysis of a low specific speed centrifugal pump, *ASME Journal of Fluids Engineering*, 139 (7) (2017) 071101.
[12] L. L. Zheng, H.-S. Dou, X. P. Chen, Z. C. Zhu and B. L. Cui, Pressure fluctuation generated by the interaction of blade and tongue, *Journal of Thermal Science*, 27 (1) (2018) 8-16.
[13] J. S. Zhang and L. Tan, Energy performance and pressure fluctuation of a multiphase pump with different gas volume fractions, *Energies*, 11 (5) (2018) 1216.
[14] N. Zhang, M. G. Yang, B. Gao, L. Zhong and N, Dan, Experimental investigation on unsteady pressure pulsation in a centrifugal pump with special slope volute, *ASME Journal of Fluids Engineering*, 137 (6) (2015) 061103.
[15] R. Spence and J. Amaral-Teixeira, Investigation into pressure pulsations in a centrifugal pump using numerical methods supported by industrial test, *Computers & Fluids*, 37 (6) (2008) 690-704.
[16] B. Gao, N. Zhang, Z. Li, D. Ni and M. G. Yang, Influence of the blade trailing edge profile on the performance and unsteady pressure pulsations in a low specific speed centrifugal pump, *ASME Journal of Fluids Engineering*, 138 (5) (2016) 051106.
[17] N. Zhang, X. K. Liu, B. Gao, X. J. Wang and B. Xia, Effects of modifying the blade trailing edge profile on unsteady pressure pulsations and flow structures in a centrifugal pump, *International Journal of Heat and Fluid Flow*, 75 (2019) 227-238.
[18] H. L. Liu, K. K. Luo, X. F. Wu, H. L. Chen and K. Wand, Effect of inlet splitter on pressure fluctuations in a double-suction centrifugal pump, *Journal of Vibroengineering*, 19 (1) 2017 549-562.
[19] K. K. Luo, Y. Wang, H. L. Liu, J. Chen, Y. Li and J. Yan, Effect of suction chamber baffles on pressure fluctuations in a low specific speed centrifugal pump, *Journal of Vibroengineering*, 21 (5) (2019) 1441-1455.
[20] Y. Tao, S. Q. Yuan, J. R. Liu, F. Zhang and J. P. Tao, The influence of the blade thickness on the pressure pulsations in a ceramic centrifugal slurry pump with annular volute, *Proceedings of the Institution of Mechanical Engineers, Part A: Journal of Power and Energy,* 231 (5) (2017) 415-431.
[21] M. Liu, L. Tan and S. L. Cao, Influence of geometry of inlet guide vanes on pressure fluctuations of a centrifugal pump, *Journal of Fluids Engineering*, 140 (9) (2018) 091204.
[22] Y. B. Liu, L. Tan, M. Liu, Y. Hao and Y. Xu, Influence of prewhirl angle and axial distance on energy performance and pressure fluctuation for a centrifugal pump with inlet guide vanes, *Energies*, 10 (5) (2017) 695.
[23] B. C. Will, F. K. Benra and H. J. Dohmen, Investigation of the flow in the impeller side clearances of a centrifugal pump with volute casing, *Journal of Thermal Science*, 21 (3) (2012) 197-208.
[24] X. Q. Jia, B. L. Cui, Y. L. Zhang and Z. C. Zhu, Study on internal flow and external performance of a semi-open impeller centrifugal pump with different tip clearances, *International Journal of Turbo & Jet-Engines*, 32 (1) (2015) 1-12.
[25] L. Cao, Y. Y. Zhang, Z. W. Wang, Y. X. Xiao and R. X. Liu, Effect of axial clearance on the efficiency of a shrouded centrifugal pump, *ASME Journal of Fluids Engineering*, 137 (7) (2015) 071101.
[26] J. R. Yan, Z. T. Zuo, W. B. Guo, H. C. Hou, X. Zhou and H. S. Chen, Influences of wear-ring clearance leakage on performance of a small-scale pump-turbine, *Proceedings of the Institution of Mechanical Engineers, Part A: Journal of Power and Energy*, 234 (4) (2019) 454-469.
[27] Y. B. Liu and L. Tan, Spatial–temporal evolution of tip leakage vortex in a mixed-flow pump with tip clearance, *ASME Journal of Fluids Engineering*, 141 (8) (2019) 081302.
[28] J. J. Feng, X. Q. Luo, P. C. Guo and G. K. Wu, Influence of tip clearance on pressure fluctuations in an axial flow pump, *Journal of Mechanical Science and Technology*, 30 (4) (2016) 1603-1610.
[29] W. Z. Zhang, Z. Y. Yu and B. S. Zhu, Influence of tip clearance on pressure fluctuation in low specific speed mixed-flow pump passage, *Energies*, 10 (2) (2017) 148.
[30] L. L. Zheng, X. P. Chen, H.-S. Dou, W. Zhang, Z. C. Zhu and X. L. Cheng, Effects of clearance flow on the characteristics of centrifugal pump under low flow rate, *Journal of Mechanical Science and Technology*, 34 (1) 2020 189-200.
[31] H. L. Liu, J. Ding, H. W. Dai and M. G. Tan, Investigation into transient flow in a centrifugal pump with wear ring clearance variation, *Advances in Mechanical Engineering*, 6 (2014) 693097.
[32] L. Cao, Y. X. Xiao, Z. W. Wang, Y. Y. Luo and X. R. Zhao, Pressure fluctuation characteristics in the sidewall gaps of a centrifugal dredging pump, *Engineering Computations*, 34 (4) (2017) 1054-1069.
[33] S. Zhang, H. X. Li and D. K. Xi, Investigation of the integrated model of side chamber, wear-rings clearance and balancing holes for centrifugal pumps, *Journal of Fluids Engineering*, 141 (10) (2019) 101101.
[34] K. A. J. Bruurs, B. P. M. van Esch and M. S. van der Schoot, Exit loss model for plain axial seals in multi-stage centrifugal pumps, *ASME 2017 Fluids Engineering Division Summer Meeting*, Hawaii (2017) V01AT05A015.
[35] K. A. J. Bruurs, B. P. M. van Esch, M. S. van der Schoot and E. J. J. van der Zijden, Axial thrust prediction for a multi-stage centrifugal pump, *ASME 2017 Fluids Engineering Division Summer Meeting*, Hawaii (2017) V01AT05A017.

**Lulu Zheng** is currently a lecturer at Henan Institute of Technology, China. He received his Ph.D. degree from Zhejiang Sci-Tech University in 2018. His main areas of interest are turbomachinery, clearance flow and computational fluid dynamics.

**Xiaoping Chen** is currently an Associate Professor at Zhejiang Sci-Tech University. He received his Ph.D. degree from University of Chinese Academy of Science in 2013. His main areas of interest are turbomachinery, turbulent flow and computational fluid dynamics.